Effect of Ce-Doping on Thermoelectric Properties in PbTe Alloys Prepared by Spark Plasma Sintering

J.Q. LI,[1,2] S.P. LI,[1] Q.B. WANG,[1] L. WANG,[1] F.S. LIU,[1] and W.Q. AO[1]

1.—Shenzhen Key Laboratory of Special Functional Materials, College of Materials Science and Engineering, Shenzhen University, Shenzhen 518060, People's Republic of China. 2.—e-mail: junqinli@szu.edu.cn

Ce-doped $Pb_{1-x}Ce_xTe$ alloys with x = 0, 0.005, 0.01, 0.015, 0.03, and 0.05 were prepared by induction melting, ball milling, and spark plasma sintering techniques. The structure and thermoelectric properties of the samples were investigated. X-ray diffraction (XRD) analysis indicated that the samples were of single phase with NaCl-type structure for x less than 0.03. The lattice parameter a increases with increasing Ce content. The lower Ce-doped samples (x = 0.005 and 0.01) showed p-type conduction, whereas the pure PbTe and the higher doped samples (x = 0, 0.015, 0.03, and 0.05) showed n-type conduction. The lower Ce-doped samples exhibited a much higher absolute Seebeck coefficient, but the higher electrical resistivity and higher thermal conductivity compared with pure PbTe resulted in a lower figure of merit ZT. In contrast, the higher Ce-doped samples exhibited a lower electrical resistivity, together with a lower absolute Seebeck coefficient and comparable thermal conductivity, leading to ZT comparable to that of PbTe. The lowest thermal conductivity (range from 0.99 W m^{-1} K^{-1} at 300 K to 0.696 W m^{-1} K^{-1} at 473 K) was found in the alloy $Pb_{0.95}Ce_{0.05}Te$ due to the presence of the secondary phases, leading to a ZT higher than that of pure PbTe above 500 K. The maximum figure of merit ZT, in the alloy $Pb_{0.95}Ce_{0.05}Te$, was 0.88 at 673 K.

Key words: PbTe semiconductor, Ce doping, thermoelectric properties

INTRODUCTION

Thermoelectrics (TEs), as one of the most promising approaches for solid-state energy conversion between heat and electricity, have become increasingly important within the last decade as the availability and negative environmental impact of fossil fuels draw increasing attention.[1] The efficiency of TE devices is determined by the dimensionless figure of merit $ZT = S^2T/\rho\kappa$, where S is the Seebeck coefficient, ρ is the electrical resistivity, T is the temperature in Kelvin, and κ is the thermal conductivity. Good thermoelectric performance requires a large value of S but small values of κ and ρ.

Among the many thermoelectric materials, lead telluride (PbTe) has been considered as a promising candidate for intermediate-temperature applications.

One of the most effective and usual methods to improve the thermoelectric performance of PbTe alloys is substitution or addition of other elements. This method can optimize the power factor and reduce the thermal conductivity to some extent and thus enhance the ZT. Tl-doped PbTe ($Tl_{0.02}Pb_{0.98}Te$) can achieve a maximum ZT of 1.3 at 673 K by enhancing the Seebeck coefficient due to the creation of resonant states close to the Fermi level without affecting the thermal conductivity.[2] The addition of excess Pb and Sb to PbTe leads to a large enhancement of the power factor, achieving a ZT of 1.4 at 673 K.[3] The substitution or addition of other elements may lead to the formation of nanodots or nanoregions, which is beneficial in terms of reducing the lattice thermal conductivity or total thermal conductivity. Substitutions of Ag and Sb for Pb in PbTe result in the compound $AgPb_mSbTe_{2+m}$, exhibiting an outstanding ZT value of 2.2 at 800 K due to the distribution of Ag-Sb nanodots in the

PbTe matrix.[4] The PbTe/Ag nanocomposite with embedded Ag-rich nanodots in the PbTe has the highest power factor of 18.78 μW cm^{-1} K^{-2} at 350 K, which can be ascribed to carrier energy filtering.[5] Recently, attention has been paid to lanthanide element doping in PbTe to improve its thermoelectric properties. Lanthanide elements in PbTe are expected to be effective donors because of their trivalent character and may strongly affect the electrical and thermal transport properties. Gd doping in PbTe decreased its electrical resistivity significantly due to the very high charge carrier mobility but didn't change much its thermal conductivity as compared with that of PbTe.[6] La doping and Ag/La co-doping of PbTe can modify the carrier concentration and thermal conductivity. The alloy $Ag_{0.05}Pb_{0.99}La_{0.01}Te$ showed a high power factor of 22 μW cm^{-1} K^{-2} and a maximum ZT of 1.2 at 720 K.[7] The thermoelectric properties of the compounds $AgPb_mLaTe_{m+2}$ have been investigated and optimized.[8] Investigation of PbTe crystal doped with Ce, for application in infrared (IR) laser and detectors, has been reported.[9] In these studies, the solubility limit of Ce in PbTe was estimated by wavelength-dispersive spectroscopy (WDS) to be 0.5 at.%. Three types of Ce-rich precipitates ($CeTe_2$, Ce_3Te_7, and Ce_2Te_5) were observed in the PbTe matrix by scanning electron microscopy (SEM) and energy-dispersive spectroscopy (EDS).[9] The Ce-rich precipitates in the PbTe matrix as secondary phases may reduce its thermal conductivity, which improves its thermoelectric properties. Since the thermoelectric properties of Ce-doped PbTe have not been studied, we investigated this area in this work.

EXPERIMENTAL PROCEDURES

The elements Pb, Te, and Ce (99.99% purity) were used as starting materials. Alloys $Pb_{1-x}Ce_xTe$ with $x = 0$, 0.005, 0.01, 0.015, 0.03, and 0.05 were melted by high-frequency induction in evacuated quartz tubes and then ball-milled into powders. The ball-milling was carried out in a planetary ball mill (QM-4F; Nanjing University, China) using a hard stainless-steel vial and balls at 200 rpm for 14 h. The weight ratio of balls to powder was 20:1, and the mill vial was evacuated and then filled with purified H_2 atmosphere to prevent oxidation of the powder during the milling process. The obtained powders were consolidated by spark plasma sintering (SPS) at 663 K for 5 min under an axial pressure of 50 MPa. The peak value of impulse was 1200 A during the SPS process. The densities, measured from the sample's geometry and mass, were 7.375 g cm^{-3}, 7.387 g cm^{-3}, 7.425 g cm^{-3}, 7.379 g cm^{-3}, 7.475 g cm^{-3}, and 7.415 g cm^{-3}, corresponding to relative densities of 90.0%, 90.1%, 90.6%, 90.0%, 91.2%, and 90.5%, for the samples of $Pb_{1-x}Ce_xTe$ with $x = 0$, 0.005, 0.01, 0.015, 0.03, and 0.05, respectively. A bar specimen with dimensions

of 12.0 mm $\times$ 5.0 mm $\times$ 5.0 mm was prepared for measurement of electrical properties and a disk specimen of ϕ12.7 mm $\times$ 2.0 mm for thermal conductivity measurement.

The phases in the samples were analyzed by x-ray diffraction using a Bruker D8 Advance SS/18 kW diffractometer with Cu K$_\alpha$ radiation and JADE 5.0 software. The Rietveld refinements of the XRD patterns were performed using Topas 3.1 software. The Seebeck coefficient (S) and electrical resistivity (ρ) of the samples were evaluated using a ZEM-2 apparatus (Ulvac-Riko, Japan) in helium atmosphere. The thermal conductivity (κ) was calculated using the equation $\kappa = \lambda C_p d$, where λ is the thermal diffusivity, C_p is the heat capacity, and d is the bulk density of the sample. The thermal diffusivity was measured by a laser flash technique (NETZSCH LFA457) in Ar atmosphere. The heat capacity was measured by differential scanning calorimetry using the standard Pyroceram 9606 as the reference. The bulk density of the sample was calculated from the sample's geometry and mass.

RESULTS AND DISCUSSION

Phase Analysis

Powder x-ray diffraction patterns for the $Pb_{1-x}Ce_xTe$ ($x = 0$, 0.005, 0.01, 0.015, 0.03, and 0.05) samples are shown in Fig. 1. These results indicate that all the samples are single phase, crystallizing in the cubic NaCl-type structure without any noticeable secondary phase. However, it is noted that the x-ray diffraction pattern of the alloy $Pb_{1-x}Ce_xTe$ shifts to lower 2θ angle as the Ce content x increases up to $x = 0.03$, but does not move as the Ce content x increases further, due to substitution of the larger Ce atom for the smaller Pb atom in the compound. The compositional dependence of the lattice parameter a for the alloy $Pb_{1-x}Ce_xTe$, obtained by Rietveld refinement, is plotted in Fig. 2. From Fig. 2, one can see that the lattice parameter a increases linearly

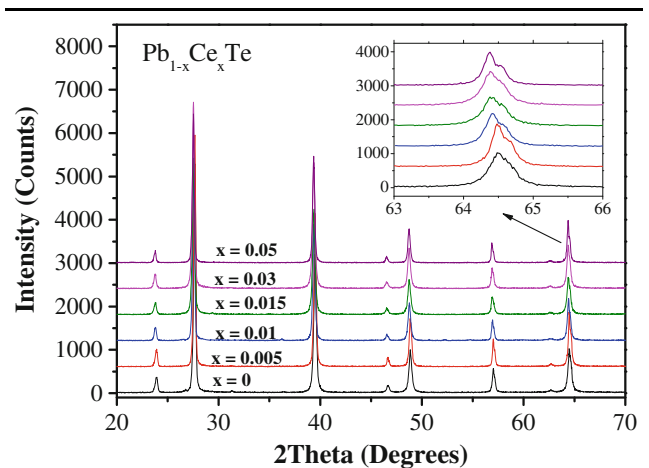Fig. 1. Powder XRD patterns for the samples of $Pb_{1-x}Ce_xTe$ with $x = 0$, 0.005, 0.01, 0.015, 0.03, and 0.05. Inset shows magnification of the selected peak near $2\theta = 65°$, showing the shift of the pattern.

with increasing Ce content up to 0.03, but changes little for the samples with x = 0.03 and 0.05. Based on the lattice parameter method, the maximum solid solubility of Ce in PbTe was estimated to be 0.022 (2.2 at.%). A minor secondary phase, in addition to the major NaCl-type structure phase, should exist in the samples of $Pb_{1-x}Ce_xTe$ with x = 0.03 and 0.05. However, the amount of the secondary phase is too small to be detected in the x-ray diffraction pattern. To identify the secondary phase(s), we increased the Ce content and prepared a sample of $Pb_{0.90}Ce_{0.10}Te$ using the same experimental condition. The powder x-ray diffraction pattern for this sample, shown in Fig. 3, reveals that the sample mainly contains the PbTe solution, together with a small amount of the compound Ce_3Te_4 and a trace of Pb. In the Ce-Te phase diagram,[10] six binary compounds, CeTe, Ce_3Te_4, Ce_4Te_7, $CeTe_2$, Ce_2Te_5, and $CeTe_3$, were
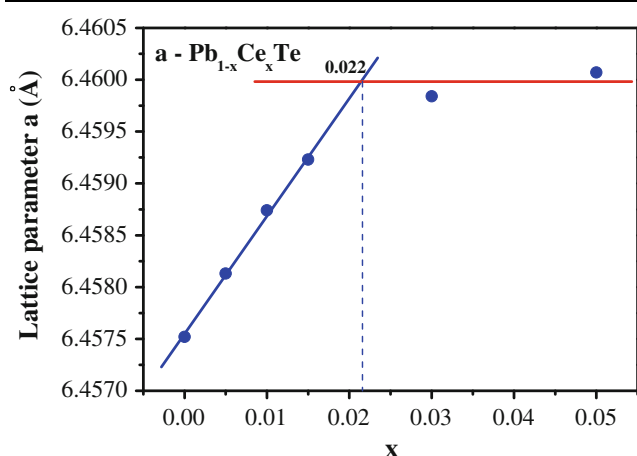
reported. The compounds CeTe and Ce_3Te_4 melt congruently at 1820°C and 1645°C, respectively, while the compounds Ce_4Te_7, $CeTe_2$, Ce_2Te_5, and $CeTe_3$ form peritectically at 1340°C, 1250°C, 870°C, and 829°C, respectively. The compound Ce_2Te_5 decomposes into $CeTe_2$ and $CeTe_3$ at 607°C. The existence of the three phases PbTe, Ce_3Te_4, and Pb in the $Pb_{0.90}Ce_{0.10}Te$ sample in this work means that the three-phase equilibrium region of PbTe + Ce_3Te_4 + Pb can be reached in the Ce-Pb-Te ternary system below 500°C, as shown in the inset to Fig. 3. Therefore, the secondary phases in the sample with x = 0.03 and 0.05 should be Ce_3Te_4 and Pb, instead of $CeTe_2$ or Ce_2Te_5. This is rather different from the compounds found in a PbTe crystal doped with Ce grown in a two-zone vertical furnace with lower-zone temperature of 850°C as reported in Ref. [9], due to the different fabrication process or different phase equilibria. The composition of the melt for PbTe crystal growth may be different in different stages. The lower heat-treatment temperature (390°C for SPS) in this work may lead to a higher maximum solid solubility (2.2 at.%) of Ce in PbTe, as compared with that of the reported PbTe crystal grown at 850°C (0.5 at.%).[9]

Thermoelectric Properties

The temperature dependence of the electrical resistivity, Seebeck coefficient, thermal conductivity, and figure of merit ZT for the alloys $Pb_{1-x}Ce_xTe$ with x = 0, 0.005, 0.01, 0.015, 0.03, and 0.05 are shown in Fig. 4. The electrical resistivities, as shown in Fig. 4a, are rather high in the lower Ce-doped samples (x = 0.005 and 0.01), being from 3.9×10^{-4} Ω m at 300 K to 3.2×10^{-4} Ω m at 673 K for $Pb_{0.99}Ce_{0.01}Te$ as an example, but are quite low in the higher Ce-doped samples (x = 0.015, 0.03, and 0.05), being from 2.1×10^{-5} Ω m at 300 K
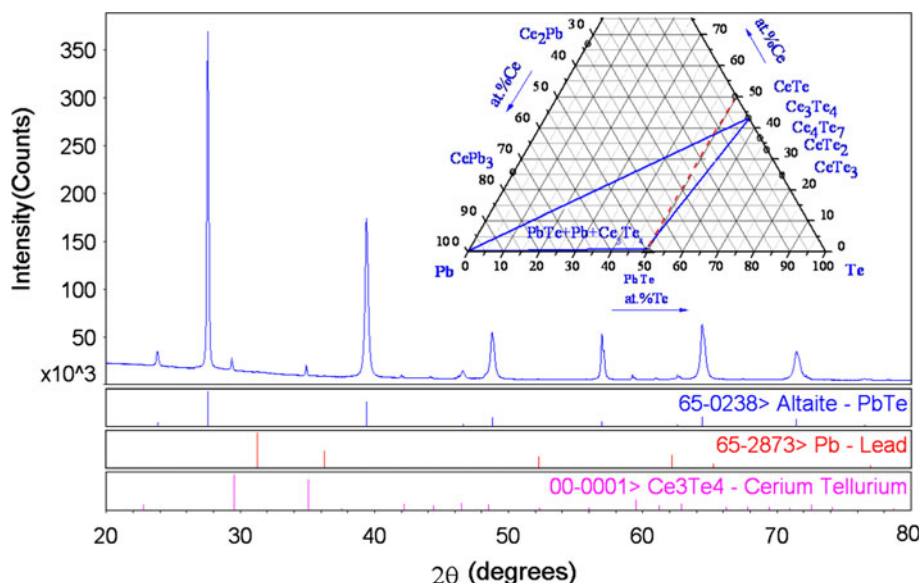

Fig. 2. Compositional dependence of the lattice parameter a for the $Pb_{1-x}Ce_xTe$ samples.

Fig. 3. Powder XRD patterns for the sample of $Pb_{0.9}Ce_{0.1}Te$. Inset shows the phase relationship for the alloys $Pb_{1-x}Ce_xTe$.
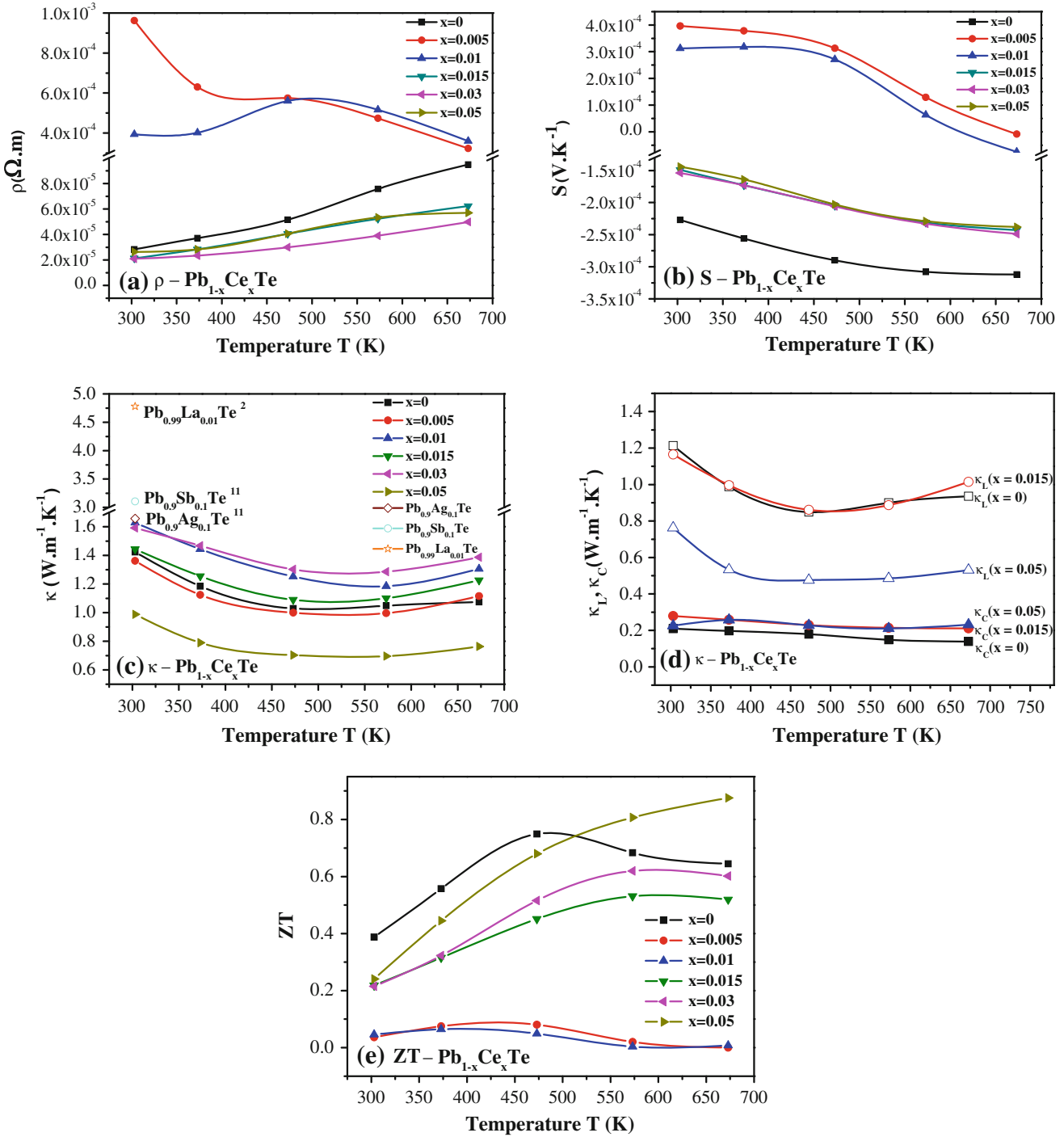
Fig. 4. Temperature dependence of the (a) electrical resistivity ρ, (b) Seebeck coefficient S, (c) thermal conductivity κ, (d) carrier thermal conductivity and lattice thermal conductivity for the representative samples, and (e) figure of merit ZT for the samples of $Pb_{1-x}Ce_xTe$ with $x = 0$, 0.005, 0.01, 0.015, 0.03, and 0.05. The total thermal conductivities for $Pb_{0.99}La_{0.01}Te$ (reported in Ref. 7), and $Pb_{0.9}Ag_{0.1}Te$ and $Pb_{0.9}Sb_{0.1}Te$ (reported in Ref. 11) at room temperature are also shown in Fig. 4c for comparison.

to 5.0×10^{-5} Ω m at 673 K for $Pb_{0.97}Ce_{0.03}Te$ as an example, as compared with that of pure PbTe from 2.8×10^{-5} Ω m at 300 K to 9.5×10^{-5} Ω m at 673 K prepared in the same condition. In a general preparation with Pb:Te = 1:1, Pb^{2+} and Te^{2-} ions form the PbTe compound, which shows n-type (electron) conduction due to the loss of a small

amount of Te by evaporation. The electrical resistivity of p-type Ag-doped PbTe is higher than that of n-type Sb-doped PbTe, mainly due to the reduction of the carrier concentration.[11] It is reasonable to believe that the electron carrier concentration is reduced in the lower Ce-doped samples but enhanced in the higher Ce-doped samples. Cerium

has three electron states: Ce^{1+}, Ce^{2+}, and Ce^{3+}. The cerium electron states belong to the stable Ce^{1+} and Ce^{3+} impurity charge states in the Ce-doped PbTe crystal prepared by the Bridgman technique, as observed by its far-infrared reflectivity spectrum.[12] The position of the pinned Fermi level and the type of conduction depend on the balance between Ce^{1+} and Ce^{3+} impurity states.[12] We believed that the Ce ion mainly adopts the Ce^{1+} state in the lower Ce-doped samples ($x = 0.005$ and 0.01) and thus the samples exhibit p-type conduction, but mainly the Ce^{3+} state in the higher Ce-doped samples ($x = 0.015$, 0.03, and 0.05), leading to n-type conduction. This was confirmed by Seebeck coefficient measurements, shown in Fig. 4b. The electrical resistivities in the higher Ce-doped samples ($x = 0.015$ and 0.03) are lower and show weaker temperature dependence compared with pure PbTe, due to their higher electron carrier concentration due to the introduction of the Ce impurity. The electrical resistivity of the Ce-doped samples $Pb_{1-x}Ce_xTe$ is on the same order as, but slightly larger than, that of the La-doped samples $Pb_{1-x}La_xTe$, since the latter were prepared by a melting process.[7]

The Seebeck coefficients for the Ce-doped samples, shown in Fig. 4b, were found to be positive for the lower Ce-doped samples exhibiting p-type conduction, but are negative for the higher Ce-doped samples with n-type conduction. As discussed above, two stable Ce^{1+} and Ce^{3+} charge states are present in the Ce-doped PbTe crystal. The Ce^{1+} ions in the PbTe lattice act as acceptors that provide hole carriers by accepting electrons from the valance band into an acceptor state above the top of the valance band. In contract, the Ce^{3+} ions in the PbTe lattice act as donors that provide electrons to the conduction band from a donor state below the conduction band. More Ce^{1+} in the lower Ce-doped samples ($x = 0.005$ and 0.01) leads to their n-type conduction, while more Ce^{3+} in the higher Ce-doped samples ($x = 0.015$, 0.03, and 0.05) leads to p-type conduction. The Seebeck coefficients are from 396 $\mu V\ K^{-1}$ at 300 K to $-8.65\ \mu V\ K^{-1}$ at 673 K for the sample with $x = 0.005$, and from 312 $\mu V\ K^{-1}$ at 300 K to $-75.2\ \mu V\ K^{-1}$ at 673 K for the sample with $x = 0.01$. This sign change may be related to the onset of intrinsic conduction and shows the superiority of electron conduction for the alloys at high temperature. Similar behavior was also reported in PbTe.[13,14] The Seebeck coefficients for the higher Ce-doped samples ($x = 0.015$, 0.03, and 0.05) were found to be negative over the entire temperature range, indicating that electron-type carriers dominate the thermoelectric transport. It is noted that the absolute Seebeck coefficients for these higher Ce-doped samples remain almost unchanged with Ce content, 150 $\mu V\ K^{-1}$ at 300 K and 200 $\mu V\ K^{-1}$ at 673 K, and lower than that of pure PbTe (230 $\mu V\ K^{-1}$ to 310 $\mu V\ K^{-1}$). It is known that the Seebeck coefficient is highly dependent on the carrier concentration. It is reasonable to believe that

the carrier concentrations for these higher Ce-doped samples should be almost the same, since the maximum solid solubility of Ce in PbTe was obtained as 2.2% by XRD. This behavior was also found in the Sb-doped PbTe sample.[11] The presence of the secondary phases may also slightly affect the Seebeck coefficient and electrical resistivity in this work.

The temperature dependence of the thermal conductivity for the samples of $Pb_{1-x}Ce_xTe$ ($x = 0$, 0.005, 0.01, 0.015, 0.03, and 0.05), shown in Fig. 4c, reveals that the thermal conductivities of all the samples firstly decrease slightly and then increase with increasing temperature. The thermal conductivity for the sample with $x = 0.005$, varying from 1.36 $W\ m^{-1}\ K^{-1}$ at 300 K to 1.0 $W\ m^{-1}\ K^{-1}$ at 473 K, is almost the same as that of pure PbTe (1.4 $W\ m^{-1}\ K^{-1}$ to 1.0 $W\ m^{-1}\ K^{-1}$) in the same experimental condition, while the thermal conductivity for the sample with higher Ce content increases with increasing x up to 0.03. However, the thermal conductivity for the sample with $x = 0.05$ is reduced to the range from 0.99 $W\ m^{-1}\ K^{-1}$ at 300 K to 0.696 $W\ m^{-1}\ K^{-1}$ at 573 K. The thermal conductivity for the Ce-doped sample $Pb_{1-x}Ce_xTe$ is lower than those of $Pb_{0.9}Ag_{0.1}Te$ (1.65 $W\ m^{-1}\ K^{-1}$ at 300 K), $Pb_{0.9}Sb_{0.1}Te$ (3.10 $W\ m^{-1}\ K^{-1}$ at 300 K),[11] or $Pb_{0.99}La_{0.01}Te$ (4.78 $W\ m^{-1}\ K^{-1}$ at 300 K) prepared by melting,[7] also shown in Fig. 4c. There are two contributions to the total thermal conductivity: the lattice part κ_L and the carrier part κ_C. κ_C can be estimated by the Wiedemann–Franz law as $\kappa_C = LT/\rho$ (Lorenz number $L = 1.96 \times 10^{-8}\ W\ \Omega\ K^{-2}$). Thus, in principle, the lattice thermal conductivity κ_L can be deduced by subtracting the carrier thermal conductivity κ_C from the total thermal conductivity κ. The temperature dependence of the carrier thermal conductivity κ_C and the lattice thermal conductivity κ_L for the representative samples $Pb_{1-x}Ce_xTe$ with $x = 0$, 0.015, and 0.05 is shown in Fig. 4d. One can see that the lattice thermal conductivity κ_L dominates the total thermal conductivity in the $Pb_{1-x}Ce_xTe$ alloys. The samples of $Pb_{0.985}Ce_{0.015}Te$ and $Pb_{0.95}Ce_{0.05}Te$ show the higher carrier (electron) thermal conductivities due to their higher carrier concentration as compared with pure PbTe. The lattice thermal conductivity κ_L for the sample of $Pb_{0.985}Ce_{0.015}Te$ is not obviously changed as compared with that of pure PbTe. However, the sample of $Pb_{0.95}Ce_{0.05}Te$ shows much lower lattice thermal conductivity than that of pure PbTe due to phonon scattering by the secondary phases Ce_3Te_4 and Pb. The reduction of the lattice thermal conductivity leads to the reduction of the total thermal conductivity.

The figures of merit (ZTs) for the samples $Pb_{1-x}Ce_xTe$ can be calculated by the equation $ZT = S^2T/\rho\kappa$, using the data shown above in the investigated temperature range. The results are shown in Fig. 4e. Although the lower Ce-doped samples ($x = 0.005$ and 0.01) show a rather high Seebeck coefficient, their high resistivity leads to

low ZT values. However, the higher Ce-doped samples ($x = 0.015$ and 0.03) have a low absolute Seebeck coefficient, but their much lower electrical resistivity leads to comparable ZT values to that of PbTe. Low thermal conductivity (range from 0.99 W m^{-1} K^{-1} at 300 K to 0.696 W m^{-1} K^{-1} at 473 K) was found in the alloy Pb$_{0.95}$Ce$_{0.05}$Te due to the presence of the secondary phases Ce$_3$Te$_4$ and Pb, leading to ZT comparable to that of pure PbTe below 500 K and higher than that of pure PbTe above 500 K. The maximum figure of merit ZT in this work, in the alloy Pb$_{0.95}$Ce$_{0.05}$Te, was 0.88 at 673 K, which is higher than that of 0.75 for pure PbTe under the same condition, 0.8 for pure PbTe fabricated by a combination of the hydrothermal method and hot pressing,[15] 0.7 for Pb$_{0.99}$La$_{0.01}$Te at 673 K,[7] and 0.27 for Pb$_{0.9}$Ag$_{0.1}$Te or 0.62 for Pb$_{0.9}$Sb$_{0.1}$Te at 723 K.[11] The TE properties for the samples of Pb$_{1-x}$Ce$_x$Te may be further optimized.

CONCLUSIONS

Ce-doped Pb$_{1-x}$Ce$_x$Te alloys were prepared, and the effects of doping on the thermoelectric properties were investigated. Substitution of Pb^{2+} ions by Ce^{1+} ions in the lower Ce-doped samples ($x = 0.005$ and 0.01) resulted in p-type conduction, reduced electrical carrier concentration, higher Seebeck coefficient, and undesired higher electrical resistivity, leading to a low figure of merit ZT. Substitution of Pb^{2+} ions by Ce^{3+} ions in the higher Ce-doped samples ($x = 0.015$, 0.03, and 0.05) caused n-type conduction, increased electrical carrier concentration, lowered electrical resistivity, and lowered absolute Seebeck coefficient, leading to ZT comparable to that of PbTe. The low thermal conductivity (range from 0.99 W m^{-1} K^{-1} at 300 K to 0.696 W m^{-1} K^{-1} at 473 K) of the alloy Pb$_{0.95}$Ce$_{0.05}$Te due to scattering of phonons by the secondary phases led to a ZT value comparable to that of pure PbTe below 500 K and higher than that of pure PbTe above 500 K.

The maximum figure of merit ZT, in the alloy Pb$_{0.95}$Ce$_{0.05}$Te, was 0.88 at 673 K.

ACKNOWLEDGEMENTS

REFERENCES

1. L.E. Bell, *Science* 321, 1457 (2008).
2. B. Yu, Q.Y. Zhang, H. Wang, X.W. Wang, H.Z. Wang, D.Z. Wang, H. Wang, G. Jeffrey Snyder, G. Chen, and Z.F. Ren, *J. Appl. Phys.* 108, 016104 (2010).
3. J.R. Sootsman, H.J. Kong, C. Uher, J.J. D'Angelo, C. Wu, T.P. Hogan, T. Caillat, and M.G. Kanatzidis, *Angew. Chem. Int. Ed.* 47, 8618 (2008).
4. K.F. Hsu, S. Loo, F. Guo, W. Chen, J.S. Dyck, C. Uher, T. Hogan, E.K. Polychroniadis, and M.G. Kanatzidis, *Science* 303, 818 (2004).
5. B. Paul, V. Ajay Kumar, and P. Banerji, *J. Appl. Phys.* 108, 064322 (2010).
6. K. Nouneh, K.J. Plucinski, M. Bakasse, and I.V.J. Kityk, *Mater. Sci.* 42, 6847 (2007).
7. K. Ahn, C.P. Li, C. Uher, and M.G. Kanatzidis, *Chem. Mater.* 21, 1361 (2009).
8. K. Ahn, C.P. Li, C. Uher, and M.G. Kanatzidis, *Chem. Mater.* 22, 876 (2010).
9. P. Fita, K. Smoliński, Z. Golacki, and K. Lawniczak-Jablonska, *Appl. Phys.* 68, 681 (1999).
10. T.B. Massalski, eds., *Binary Alloy Phase diagram*, Vol. 2 (Metals Park, OH: American Society for Metals, 1990), p. 1118.
11. H.S. Dow, M.W. Oh, B.S. Kim, S.D. Park, B.K. Min, H.W. Lee, and D.M. Wee, *J. Appl. Phys.* 108, 113709 (2010).
12. P.M. Nikolić, K.T. Radulović, S.S. Vujatović, D. Vasiljević-Radović, S. Đurić, V. Blagojević, P. Mihajlović, D. Urošević, Z. Dohčević-Mitrović, and O. Jakšić, *J. Optoelectron. Adv. Mater.* 2, 465 (2000).
13. H. Li, K.F. Cai, H.F. Wang, L. Wang, J.L. Yin, and C.W. Zhou, *J. Solid State Chem.* 182, 869 (2009).
14. M. Orihashi, Y. Noda, L.D. Chen, T. Goto, and T. Hirai, *J. Phys. Chem. Solids.* 61, 919 (2000).
15. Y.Q. Cao, T.J. Zhu, and X.B. Zhao, *J. Phys. D: Appl. Phys.* 42, 015406 (2009).